

Spatial and Temporal Patterns of Winter–Spring Oxygen Depletion in Chesapeake Bay Bottom Water

Jeremy M. Testa · W. Michael Kemp

Received: 16 July 2013 / Revised: 6 January 2014 / Accepted: 12 January 2014 / Published online: 28 April 2014
© Coastal and Estuarine Research Federation 2014

Abstract Although seasonal hypoxia is a well-studied phenomenon in many coastal systems, most previous studies have only focused on variability and controls on low-oxygen water masses during warm months when hypoxia is most extensive. Surprisingly, little attention has been given to investigations of what controls the development of hypoxic water in the months leading up to seasonal oxygen minima in temperate ecosystems. Thus, we investigated aspects of winter–spring oxygen depletion using a 25-year time series (1985–2009) by computing rates of water column O₂ depletion and the timing of hypoxia onset for bottom waters of Chesapeake Bay. On average, hypoxia (O₂ <62.5 μM) initiated in the northernmost region of the deep, central channel in early May and extended southward over ensuing months; however, the range of hypoxia onset dates spanned >50 days (April 6 to May 31 in the upper Bay). O₂ depletion rates were consistently highest in the upper Bay, and elevated Susquehanna River flow resulted in more rapid O₂ depletion and earlier hypoxia onset. Winter–spring chlorophyll *a* concentration in the bottom water was highly correlated with interannual variability in hypoxia onset dates and water column O₂ depletion rates in the upper and middle Bay, while stratification strength was a more significant driver in the timing of lower Bay hypoxia onset. Hypoxia started earlier in 2012 (April 6) than previously recorded, which may be related to unique climatic and biological conditions in the winter–spring of 2012, including the potential carryover of organic matter delivered to the system during a tropical storm in September 2011. In general, mid-to-late summer hypoxic volumes were not correlated

to winter–spring O₂ depletion rates and onset, suggesting that the maintenance of summer hypoxia is controlled more by summer algal production and physical forcing than winter–spring processes. This study provides a novel synthesis of O₂ depletion rates and hypoxia onset dates for Chesapeake Bay, revealing controls on the phenology of hypoxia development in this estuary.

Keywords Oxygen · Hypoxia · Chlorophyll *a* · Stratification

Introduction

Seasonal depletion of dissolved oxygen (O₂) from coastal waters is a widespread phenomenon that appears to be growing globally (Díaz and Rosenberg 2008; Rabalais and Gilbert 2009). There is mounting evidence that eutrophication is contributing to the expansion of occurrence, intensity, and duration of hypoxic (“hypoxia”=O₂<62.5 μM, 2 mg l⁻¹, 30 % saturation) conditions in coastal waters worldwide (Díaz and Rosenberg 2008; Kemp et al. 2009). Short- and long-term patterns and trends in climatic forcing, however, also exert control over O₂ in bottom waters (Justic et al. 2005; Scully 2010; Wilson et al. 2008). Considering the potential impacts of hypoxia on the behavior, growth, and mortality of many marine fish and invertebrates (Brady et al. 2009; Vaquer-Sunyer and Duarte 2008); predator–prey interactions and food web structures (Decker et al. 2004; Nestlerode and Diaz 1998); and biogeochemical processes (Conley et al. 2002; Kemp et al. 1990; Testa and Kemp 2012), this phenomenon has received increasing attention in recent decades.

It is well known that O₂ concentrations are gradually depleted from deeper waters of Chesapeake Bay from late winter until early summer, resulting in the hypoxic and anoxic conditions that persist from mid-June–September (Hagy et al. 2004). O₂ concentrations usually reach their seasonal peak in January–February, when solubility is high, vertical mixing strong, and O₂ consuming processes are temperature-limited (Taft et al.

Communicated by Dennis Swaney

J. M. Testa (✉)
Chesapeake Biological Laboratory, University of Maryland Center
for Environmental Science, Solomons, MD 20688, USA
e-mail: jtesta@umces.edu

J. M. Testa · W. M. Kemp
Horn Point Laboratory, University of Maryland Center for
Environmental Science, Cambridge, MD 21613, USA

1980). Beginning in February and March, O₂ concentrations in deeper water (>10 m) tend to follow a relatively linear decline until June at rates ranging from ~1 to 5 mmol O₂m⁻³ day⁻¹ (Boynton and Kemp 2000). Such rapid O₂ declines lead to the onset of hypoxic and anoxic conditions as early as April and June, respectively, near the head of the hypoxic zone (39°N, -76.3°W). As the summer progresses, hypoxic conditions expand southward, reaching as far south as 37.5°N by July.

Previous studies have suggested that the rate of spring O₂ decline and the onset of hypoxia are highly variable from year to year (Boynton and Kemp 2000; Hagy et al. 2004). It has been suggested that such high interannual variability in the seasonal development of O₂-depleted bottom waters is driven by a suite of biological and physical variables, including the magnitude of the spring diatom bloom, spring water temperature, and winter–spring river flow and wind conditions (Boynton and Kemp 2000; Hagy et al. 2004; Officer et al. 1984; Scully 2010). The response of O₂ depletion to these various drivers is almost certainly nonlinear. For example, elevated winter–spring river flow should favor O₂ depletion by increasing vertical stratification and reducing vertical mixing (Boicourt 1992), and by elevating phytoplankton growth (Malone et al. 1988). Higher river flow will, however, limit O₂ depletion by enhancing landward, longitudinal inputs of O₂ (Kemp et al. 1992; Kuo et al. 1991) and pushing spring bloom phytoplankton biomass to seaward regions of the Bay (e.g., Hagy et al. 2005).

Despite the high variability and potential importance of hypoxia initialization in spring, most of the hypoxia research in Chesapeake Bay has focused on the summer (June–August) period when the volume of hypoxia is at its seasonal peak (Hagy et al. 2004; Murphy et al. 2011; Scavia et al. 2006). In part, this summer focus is due to the availability of historical O₂ data (1950–1980, Hagy et al. 2004) and an emphasis on summer hypoxic effects on living resources (Breitburg 2002). Consequently, the spatial and temporal patterns in the development of hypoxia during spring and the processes that control these patterns are poorly understood. This is an important gap in understanding for a number of reasons, including the fact that previous investigators have suggested that the spring bloom is the primary source of organic matter driving respiration and summer hypoxia (e.g., Malone 1987; Pomeroy et al. 2006). Although previous studies have addressed questions on the magnitude and controls on spring O₂ depletion (Boynton and Kemp 2000; Hagy et al. 2004; Taft et al. 1980), a comprehensive analysis of spatial and temporal patterns has heretofore been lacking.

The objective of this study was to utilize a large and spatially and temporally resolved dataset for O₂ concentrations (and other key variables) to understand the dynamics of seasonal hypoxia development in Chesapeake Bay. We used concentration time series along the Bay axis to compute rates of water column O₂ uptake, the date of hypoxia initiation, and the volume of hypoxia. Regional and seasonal variations in these processes were

also examined. Variations in these rates and dates were related to a suite of physical and biological variables and to summer hypoxia extent, providing a basis for understanding key controls over space and time.

Methods

Vertical Profiles of Concentrations

Vertical profiles of O₂, water temperature, salinity, and chlorophyll *a* were obtained from the Chesapeake Bay Program Water Quality database for the 1985–2009 period (http://www.chesapeakebay.net/data_waterquality.aspx), with profiles collected at 20 stations located along the estuary's central channel (Fig. 1, Table 1). Measurements of O₂, temperature, and salinity were generally made at 1-m depth intervals, while measurements of chlorophyll *a* were made at 4–5 depths for each station (2–10 m intervals). Profiles were generally sampled monthly between November and March and bimonthly between April and October.

Climatic Data

Daily Susquehanna River flow into the Chesapeake Bay was obtained from the USGS Chesapeake Bay River Input Monitoring Program website for the years 1985 to 2009 (<http://va.water.usgs.gov/chesbay/RIMP/>). Wind direction and speed were collected from the Patuxent Naval Air Station (PNAS) near the mouth of the Patuxent River in Maryland (Fig. 1). The PNAS data were used because they represent the most centrally located site relative to the main stem of the bay. The wind direction was calculated from the hourly north and east wind components after the data are filtered with a 36-h low-pass filter. In computing average wind speeds, only those records where wind blew with a speed greater than 2 m s⁻¹ were used. Wind directions were categorized into eight compass directions (e.g., Murphy et al. 2011).

Stratification

We computed pycnocline depth for each region as the vertical position in the water column (depth (meter), *z*) where the square of the Brunt–Väisälä frequency (*N*²) was at its maximum value (e.g., Pond and Pickard 1983) and that value was used as an index of pycnocline strength, where

$$N^2(z) = \frac{g}{\sigma_z} \cdot \frac{\partial \sigma}{\partial z}$$

and *g*=gravitational constant, 9.81 m s⁻², σ_z is the water density at depth (in kilogram per cubic meter), and $\frac{\partial \sigma}{\partial z}$ is the density gradient at depth *z*, which was calculated using a 2-m window

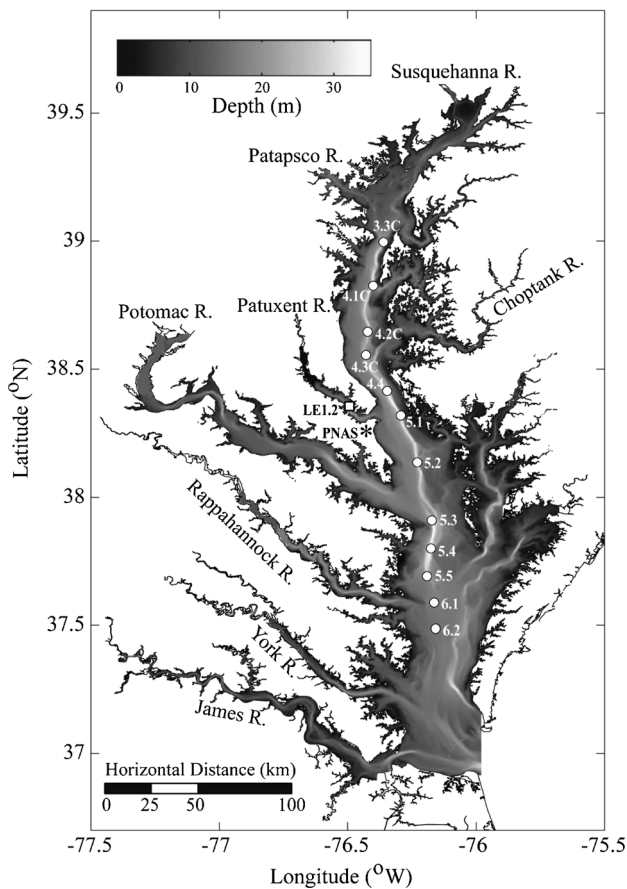


Fig. 1 Map of Chesapeake Bay with bathymetry (see “Depth” key) and major tributaries included (also note horizontal “Distance” key). Circles indicate the location of monitoring stations, where the “CB” prefix to each number have been omitted. Open square indicates the location of station LE1.2, where continuous observations of dissolved O_2 were made. Asterisk indicates the location of the Patuxent River Naval Air Station (PNAS)

around z . Density was computed from profiles of temperature and salinity data (Fofonoff 1985) at 1-m depth intervals using the Chesapeake Bay Program Water Quality database.

Interpolations

We interpolated spatial distributions for O_2 , water temperature, salinity, and chlorophyll a concentrations to a 2D length–depth grid using ordinary kriging (Murphy et al. 2010; Murphy et al. 2011). The statistical package R (R Development Core Team 2009) with the geoR package (Ribeiro and Diggle 2009) was used for all interpolations (Murphy et al. 2011). The resulting 2D distributions were assumed to be constant laterally at a given depth and organized to correspond to tabulated cross-sectional volumes (Cronin and Pritchard 1975). For O_2 , interpolated concentration data were multiplied by the cross-sectional volumes to compute “hypoxic volumes” for all available profile sets in the

years 1985–2009 by summing the volume of all cells with an O_2 concentration $<62.5 \mu\text{M}$.

O_2 Depletion Metrics

The first day of the year where bottom water O_2 concentrations fall below $62.5 \mu\text{M}$ provides the most straightforward index of the tendency for hypoxia to occur in a given year. This date was calculated by (1) averaging bottom water O_2 concentrations for each sampling date, (2) interpolating temporally through time to extrapolate fortnightly and monthly data to a daily concentrations using shape-preserving piecewise cubic interpolations (i.e., the interpolation is monotonic when data are monotonic and no artificial maxima or minima are generated; Fritsch and Carlson 1980), and (3) calculating the day where interpolated O_2 fell below $62.5 \mu\text{M}$ (Fig. 2). Hypoxia onset dates were calculated for each station in each year from 1985 to 2009.

The rate of O_2 depletion was calculated as the slope of a linear temporal decline in O_2 concentration (non-interpolated) between March and May for each year between 1985 and 2009. Because maximum depth varies by station (Table 1), the O_2 concentrations used were from the deepest depth sampled at a particular station, which does not generally vary by more than 1 m. For each year and station, the slope was calculated by a linear regression model fit to the March–May time series of averaged O_2 concentrations versus time (Fig. 2). The slope represents a daily O_2 depletion rate, and it reflects the effects on O_2 of various biological, physical, and chemical mechanisms. We made the same computations on time series of O_2 deficit ($O_{2\text{Saturation}} - O_{2\text{Observed}}$) to examine the impacts of changes in solubility (driven primarily by temperature) on our depletion rates (data not shown); these slopes were highly correlated with the slopes from the observations ($r > 0.90$). For a few years, the O_2 time series from March to May was not linear (Fig. 3). This nonlinearity was most often the result of a single, short-term (daily to weekly) increase in concentration due to landward advection or vertical mixing of high- O_2 water (e.g., Fig. 4). Correlation coefficients (r values) for the linear model fits to observed concentrations generally exceeded 0.90 at all stations/sites.

Data used in this analysis, which are based on routine measurements at 2–4 week intervals, are likely to miss some short-term (i.e., hourly–daily) dynamics in O_2 concentrations. Continuous dissolved O_2 measurements (sampling at 15-min intervals) were made from a fixed buoy deployed adjacent to a routine monitoring station in the lower Patuxent estuary (LE1.2) during spring of 2004 (Figs. 1 and 4; Alliance for Coastal Technologies (ACT), <http://www.act-us.info/>). Comparisons of these two datasets reveal how different scales of O_2 variability are captured by the two sampling intervals. Rate of O_2 depletion (ROD) and date of hypoxia onset (DHO) calculated from these two datasets (i.e., LE1.2 and ACT) over the April to May period

Table 1 Monitoring station characteristics and hypoxia metrics in the modern (1985–2009) Chesapeake Bay Program-MD Department of Natural Resources dataset

Station	Latitude	Longitude	Depth (m)	Surface salinity	Hypoxia onset	% years hypoxic	O ₂ depletion rate (mmol O ₂ m ⁻³ day ⁻¹)
CB3.3C	38.996	-76.359	26	9.13	May 4 (±13)	100	3.19 (±0.78)
CB4.1C	38.826	-76.399	33	10.77	May 8 (±15)	100	3.16 (±0.63)
CB4.2C	38.646	-76.421	28	11.82	May 17 (±16)	100	3.34 (±0.69)
CB4.3C	38.555	-76.428	28	12.15	May 19 (±17)	100	3.31 (±0.63)
CB4.4	38.415	-76.346	32	12.90	May 23 (±18)	100	3.16 (±0.75)
CB5.1	38.319	-76.292	36	13.55	May 24 (±18)	100	3.09 (±0.91)
CB5.2	38.137	-76.228	33	14.08	June 1 (±17)	100	2.94 (±0.78)
CB5.3	37.910	-76.171	29	14.38	June 19 (±20)	100	2.66 (±0.59)
CB5.4	37.800	-76.175	34	16.46	June 22 (±26)	96.0	2.38 (±0.72)
CB5.5	37.692	-76.189	21	16.71	June 30 (±23)	84.0	2.44 (±0.75)
CB6.1	37.589	-76.162	13	17.55	July 5 (±13)	76.0	2.09 (±0.72)
CB6.2	37.487	-76.156	14	18.06	July 20 (±27)	52.0	1.88 (±0.84)

See Fig. 1 for map with station locations within Chesapeake Bay. Surface salinity, date of hypoxia onset, and rate of water column O₂ depletion are means (±SD) over 1985–2009 period

are similar, despite the fact that several multi-day periods of high variability in O₂ occurred between the fortnightly samples (where the fortnightly samples are similar to those used for the majority of calculations in this study; Fig. 4). High-frequency data (15-min) were not available for the mainstem Bay, where we focused our study.

Statistical Analysis

We investigated the potential for multiple interacting controls on the DHO and the ROD using simple linear regression and multiple linear regression models (SASv9.2, PROC REG). The independent variables used to construct the models included mean January to May Susquehanna River flow, March–May wind speed and direction, January to April bottom water chlorophyll *a*, March to May water temperature, and April and May pycnocline strength (N^2) and vertical position (depth of maximum N^2). The chosen periods of aggregation for river flow and chlorophyll *a* include 1–2 months prior to the time of the O₂ depletion calculations, as these drivers may have delayed effects, while wind and stratification metrics, which have more immediate impacts on O₂, were aggregated during the period of analysis. Three multiple linear regression approaches were used, including r^2 selection of all predictor sets, forward selection, and backward selection. Selection of optimal models was based on maximizing the adjusted r^2 of the model and minimizing the Mallows' CP and Akaike information criterion. We tested for normality of residuals using Shapiro–Wilk's W and box and normal probability plots. Multicollinearity of predictor variables was examined via variance inflation, condition indexes,

and eigenvalues of predictor variables. We used correlation analysis to compare estimates of DHO and ROD to estimated volumes of hypoxia made for latter-month (the second of two monthly cruises) data for May to August cruises.

Results

Temporal and Spatial Patterns in O₂

Bottom water-dissolved O₂ varies seasonally in Chesapeake Bay, with maximum values in February and minimum concentrations typically occurring between May and August (Fig. 3). In most summers, anoxic concentrations occur in upper and middle Bay stations (CB3.3C to CB5.2), while hypoxic or near-hypoxic concentrations occur in the lower Bay (e.g., CB6.2) and anoxia is rare (Fig. 3). Time series of bottom water O₂ at the northern and southern ends of the hypoxic zone stations illustrate consistent seasonal patterns with moderate interannual variability in O₂ minima and episodic O₂ replenishment during summer in some years (e.g., 1988 in Fig. 3).

The 25-year (1985–2009) monthly mean (March–July) spatial distributions in dissolved O₂ reveal the development of hypoxic water over the March–May period, as well and the seaward spread of low-O₂ water along the Bay axis during spring (Fig. 5a). Parallel time/space patterns in the variance around these mean conditions are also revealing (Fig. 5b). O₂ first begins to decline in bottom water within the upper Bay between 200 and 300 km from the Atlantic Ocean in March–April (Fig. 5a). From

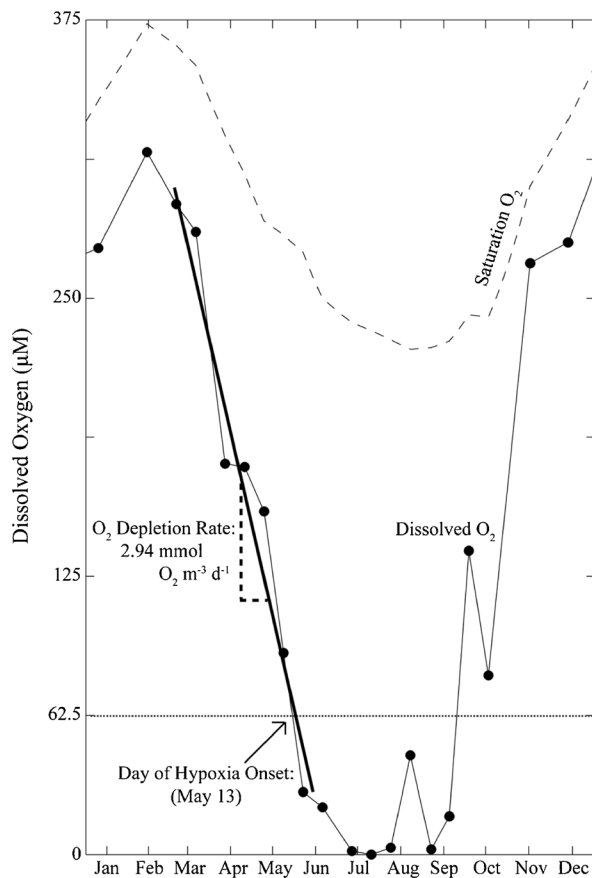


Fig. 2 Seasonal cycle of bottom water O_2 saturation and concentration at CB5.1 (Fig. 1) in 2004 and illustration of how rate water column O_2 depletion and date of hypoxia onset were derived from the time series data (see text)

this location, O_2 further declines through June and the location of the low- O_2 water mass appears to migrate seaward over the course of spring, where it is generally retained below 10–12 m depth (Fig. 5a). The standard deviation in O_2 around these 25-year means also reveals both spatial and seasonal shifts in O_2 variability. In March and April, O_2 is most variable in the upper Bay where O_2 is initially depleted and where vertical gradients in O_2 concentration are strong (Fig. 5b). In contrast, O_2 variability is highest in the middle of the water column in May and June (in the vicinity of the pycnocline) throughout most of the central channel of the Bay (Fig. 5b). The standard deviation reaches a seasonal and regional peak near the mid-Bay pycnocline in June, where vertical gradients in O_2 are also at seasonal peaks.

Hypoxia Onset (DHO) and O_2 Depletion Rates (ROD)

The estimated DHO was highly variable from year to year at a given station, but the spatial pattern was consistent. For example, at station CB3.3C near the Bay Bridge (Fig. 1), the date that O_2 fell below 62.5 mM ranged from April 14 to May

31 (46 days) between 1985 and 2009, but hypoxia always initiated here before it arrived at other stations further south (Fig. 6a). Each year from 1985 to 2009, hypoxia developed in the most landward bottom waters of the Bay (near CB3.3C in Fig. 1), but in only half of those 25 years did hypoxia develop as far south as the mouth of the Rappahannock River (CB6.1). After initiating at station CB3.3C, hypoxia gradually developed at seaward stations over the ensuing 4 months, reaching the Rappahannock River by late June/early July (Fig. 6a). The median time it took hypoxia to expand from CB3.3C to CB5.5 was 58 days, although in some years, the travel time was in excess of 3 months. The latest DHO recorded was on September 17, 1991 at station CB6.2. Although the spatial pattern in DHO was relatively unchanged in high- versus low-flow years, differences between high and low Susquehanna River flows were greater north of the Potomac River (CB3.3C to CB5.2) than south (CB5.3 to CB6.2; Fig. 7). When DHO data were divided into two groups (five highest and five lowest Susquehanna River flow years), hypoxia initiated 15–25 days earlier in the years of highest flow than in the lowest flow years, while DHO was significantly earlier in the high-flow years at stations CB3.3C–CB4.3C and CB5.3 ($p < 0.05$, Mann–Whitney U test; Fig. 7a).

The water column O_2 depletion rates computed in this study were comparable to those made in previous studies using a similar approach in Chesapeake Bay at select locations (Table 2). Overall, interannual variability in the ROD was relatively greater than that of hypoxia initiation, but the spatial patterns and flow responses were similar. Whereas DHO was earlier in landward regions of the Bay, O_2 depletion rates were higher in this region (Fig. 6). Median water column O_2 depletion rates were similar north of the Potomac River (CB3.3C to CB5.2) but declined in seaward regions and ROD at stations CB3.3–CB5.1 was significantly higher than CB6.1–CB6.2 ($p < 0.05$, ANOVA with Scheffe test). O_2 depletion rates were generally insensitive to Susquehanna River flow in the upper (CB3.3C–CB4.1C) and lower Bay stations (CB5.3–CB6.4), but rates were elevated (by 30 %) in high-flow years in middle Bay regions (CB4.2C–CB5.2; Fig. 7b). No significant differences were detected between the means when O_2 depletion rates were divided into two groups based on Susquehanna River flow ($p > 0.05$, Mann–Whitney U test; Fig. 7b), although p values were less than 0.2 at stations CB4.2C to CB5.2. The highest ROD recorded was 5.31 $\text{mmol m}^{-3} \text{day}^{-1}$ at station CB5.4 in 2003.

Winter–spring chlorophyll a concentrations explained more variability in DHO and ROD than physical variables in upper and middle Bay regions (Tables 3 and 4). Although Susquehanna River flow was significantly correlated with DHO and ROD during several winter–spring periods (Tables 3 and 4), we sought explanatory variables that were more proximal to biological or physical processes. Bottom water chlorophyll a concentrations averaged over the January

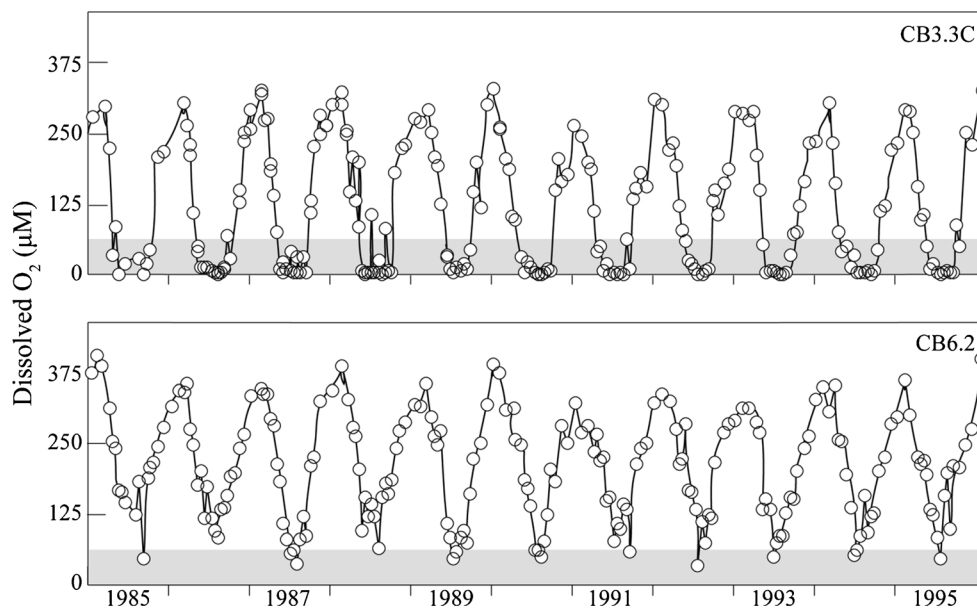


Fig. 3 Time series of bottom water O₂ concentration at two stations near the upper (CB3.3C) and lower ends of the Chesapeake Bay hypoxic zone over 1985–1995. Gray shaded area indicates the hypoxia concentration threshold (62.5 µM)

to April period were significantly and negatively correlated to DHO ($r=-0.47$ to -0.73 , $p<0.05$; CB4.1C–CB5.2) and positively related to ROD ($r=0.43$ to 0.51 , $p<0.05$; CB4.2C–CB5.2). In contrast, the Brunt–Väisälä frequency was significantly and negatively correlated to DHO in only lower Bay stations ($r=-0.43$ to -0.78 , $p<0.05$; CB5.2–CB5.4) and was positively correlated to ROD at select lower Bay stations (Table 4).

Multiple linear regressions resulted in improved predictability of DHO and ROD at only 2 of the 12 stations examined (CB4.3C and CB5.2), given the variables we included in the analysis (e.g., Fig. 8). For example, at station CB5.2, both January to April bottom water chlorophyll *a* and April to May mean Brunt–Väisälä frequency (maximum value in the water

column) were significant predictors of DHO (Fig. 8). For the majority of stations, however, only a single predictor variable explained a significant fraction of variability in the O₂ depletion metrics (Tables 3 and 4). Mean wind speed, wind direction, water temperature, and pycnocline depth were not significantly correlated ($p>0.1$) to interannual variability in DHO or ROD.

Winter–Spring O₂ Depletion and Summer Hypoxic Volume

One of the motivating questions in this effort was to understand the relationship between winter–spring O₂ depletion and summer hypoxic volume. That is, does the onset and spatial distribution of hypoxia in spring predetermine and thus predict the summer condition? We calculated the correlation between DHO and ROD and Bay-wide hypoxic volumes computed for May, June, and July (Fig. 9). DHO and ROD were weakly correlated with hypoxic volume during the mid- and late-summer ($p<0.05$; late July and August; August data not shown) period, but were significantly correlated to May, and to a lesser extent, June hypoxic volumes ($p<0.05$; Fig. 9). DHO and ROD at CB4.3C to CB5.4 were most strongly correlated to May and June hypoxic volumes, while these metrics at upper and lower Bay stations correlated weakly with hypoxic volume during May and June (Fig. 9).

Winter–Spring O₂ Depletion in 2012

In September of 2011, precipitation associated with Tropical Storm Lee (hereafter TS Lee) resulted in extraordinarily high Susquehanna River flow and suspended sediment loading rates to Chesapeake Bay. The peak Susquehanna flow

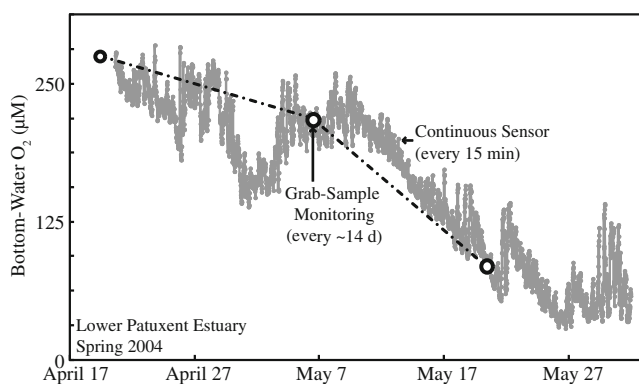


Fig. 4 Comparison of 6-week time series of bottom water O₂ (16 m deep) measured continuously (YSI data sonde every 15 min, small gray lines and circles) and measured fortnightly (14 days, open circles/dashed line) at a station in the lower Patuxent River estuary in the spring of 2004 (Station LE1.2, 38.38°N, -76.51°W, see Fig. 1)

following Tropical Storm Lee was $22,031 \text{ m}^3 \text{ s}^{-1}$ (Cheng et al. 2013), which was the largest flow since Tropical Storm Agnes in June 1972 ($\sim 32,000 \text{ m}^3 \text{ s}^{-1}$) and is about 18 times the average annual flow. Flow resulting from TS Lee was estimated to scour $3.6 \times 10^9 \text{ kg}$ of sediment from the lower Susquehanna River reservoirs (<http://chesapeake.usgs.gov/featuresedimentscourconowingo.html>) delivering this and other material to Chesapeake Bay. During the subsequent winter–spring (2012), hypoxia onset in the upper Bay occurred earlier than previously recorded in the available monitoring data (Fig. 10), as water column O_2 concentrations were at record-low levels (Fig. 11b, c). This record DHO (April 6)

was much earlier than expected from January to April mean bottom water chlorophyll a at stations CB3.3C and CB4.1C, given patterns from the previous decades (Fig. 10). Such early-season depression of O_2 may have been driven by respiration of organic matter delivered during the storm and retained in the upper Bay over the winter. In addition, record-high bottom water temperatures were observed in the winter–spring of 2012 (Fig. 11a), and April particulate organic carbon (POC) and chlorophyll a concentrations (Fig. 11d) were 1.5–2 times the long-term mean at these stations. Stratification strength was also relatively high during the winter of 2011–2012, where maximum N^2 at CB4.1C was 0.015 and 0.01 s^{-2}

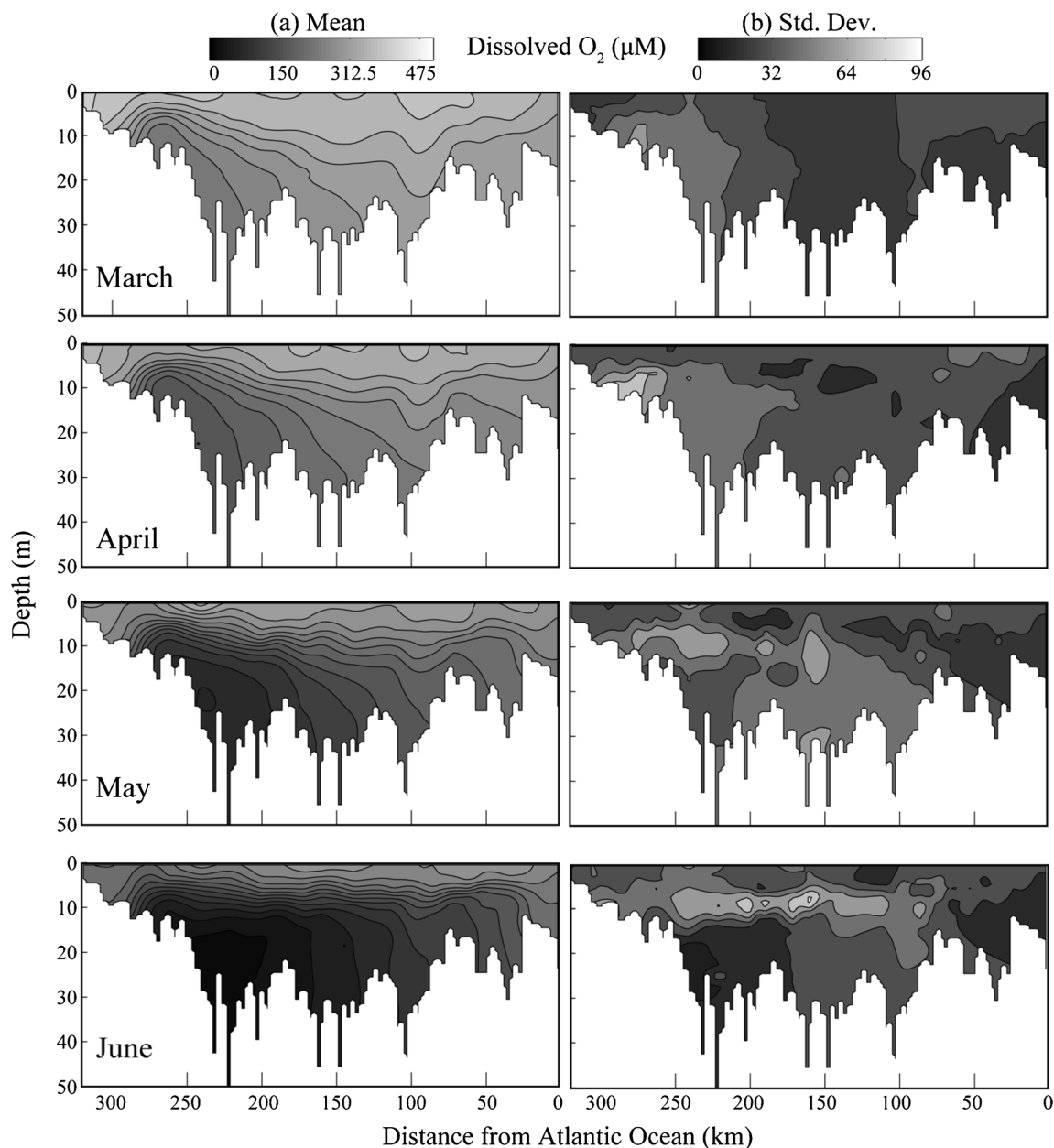


Fig. 5 Two-dimensional isopleths depicting distributions of dissolved O_2 concentration with depth and distance along the Bay axis over the years 1985–2009 for 4 months (March, April, May, June) for the 25-year mean values (a) and standard deviations around the means (b)

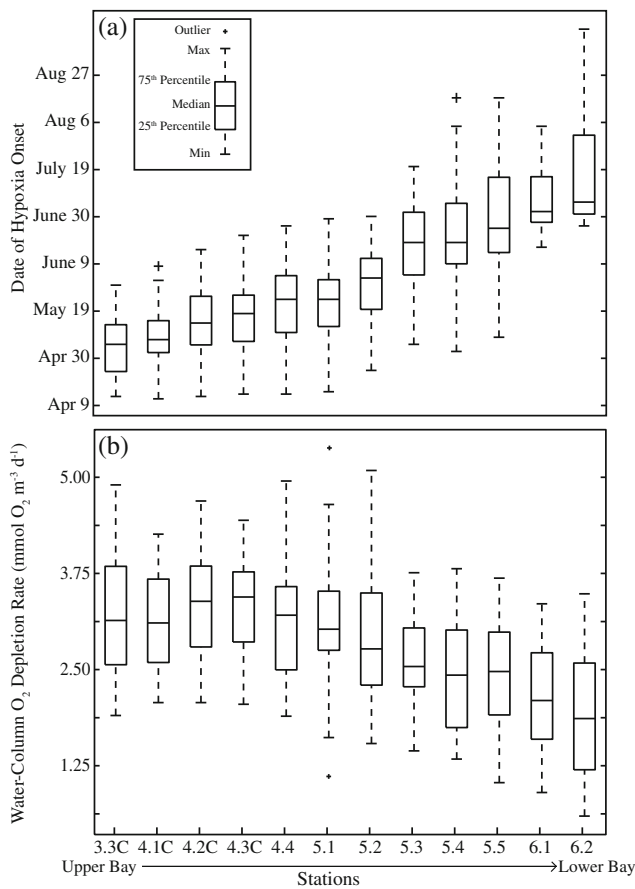


Fig. 6 Box plots of hypoxia onset day (a) and water column O₂ depletion rate (b) at 12 stations along the Chesapeake Bay axis for the years 1985 to 2009 (see Fig. 1)

in February and March, respectively, which is near the long-term (1985–2009) maxima for these months.

Discussion

Spatial and Temporal Patterns of O₂ Depletion

Although ROD, DHO, and seasonal O₂ concentration minima varied spatially in Chesapeake Bay, the pattern of decline in bottom water O₂ concentrations over the winter–spring period was generally consistent across stations along the Bay’s longitudinal axis. This pattern is well-described and reflects the combined effects of elevated temperature and associated solubility declines, respiration of spring bloom-generated algal material, and reduced ventilation caused by winter–spring river flows (Boynton and Kemp 2000; Hagy et al. 2004; Taft et al. 1980). A striking regional pattern in O₂ decline is the consistent early development of *anoxia* in the upper Bay stations, but only occasional and short-lived *hypoxia* in the lower Bay stations (Fig. 3). This results from autochthonous

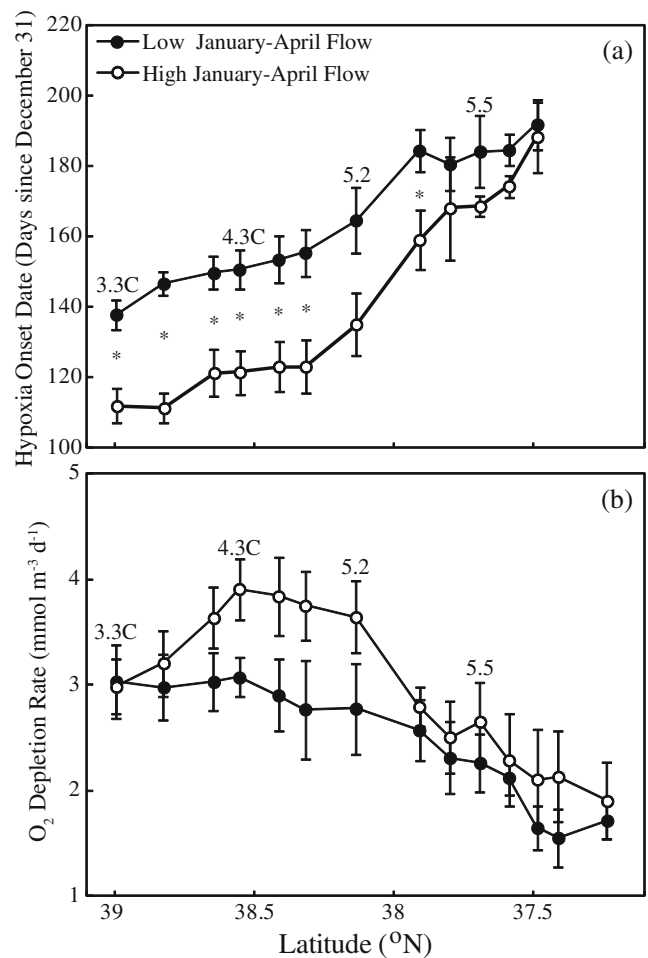


Fig. 7 Patterns of date of hypoxia onset (a) and rate of water column O₂ depletion (b) shown as mean values (± standard errors) for the 5 years of highest (open circles) and 5 years of lowest (closed circles) winter–spring Susquehanna River flow. Asterisks between lines indicate significant differences between high-flow and low-flow groups

and allochthonous organic material that accumulates in the upper and middle Bay regions in spring (Hagy et al. 2005; Zimmerman and Canuel 2001). Additionally, gravitational circulation limits the oxygenation of upper and middle Bay bottom water via two mechanisms, including (1) reduced exchange with oxygenated surface waters vertical mixing and lateral advection/mixing (Malone et al. 1986; Scully 2010) and/or (2) limited O₂ inputs via landward longitudinal advection (Kemp et al. 1992; Kuo et al. 1991). Thus, spatial patterns in winter–spring O₂ depletion are driven by a combination of biological and physical processes.

Although these declines in O₂ concentration were apparently gradual when analyzing monthly to fortnightly data, higher frequency measurements reveal that this general decline may be occasionally interrupted by brief events of both rapid depletion and ventilation (Fig. 4). Diel variability in these data suggests tidal-mixing effects (Fig. 4), but day-to-week variability is driven by wind-mixing events. For example, O₂ increases from April 28 to May 4 (Fig. 4) are

Table 2 Comparisons of rates of water column O₂ depletion from this study with previously estimated rates using several approaches

Approach	Months	Years	O ₂ depletion rate	Source
Slope of spring decline	March–May	1985–2009	0.63–5.31	This study
Slope of spring decline	February–June	1964–1977	1.25–4.69	Taft et al. (1980)
Slope of spring decline	March–May	1985–1992	2.50–5.00	Boynton and Kemp (2000)
Slope of spring decline	Not Reported	1985–2001	2.34–6.13	Hagy et al. (2004)
Residual of process budget	March–May		1.88–4.06	Kemp et al. (1992)

O₂ depletion rates are in units of millimole O₂ per cubic meter per day

associated with parallel salinity decreases, indicating downward mixing of high-O₂ and low-salinity water. Although it is likely that such high frequency variability also characterizes the time series in the main channel of Chesapeake Bay (Boicourt 1992; Breitburg 1990), limited data exist to sufficiently examine this variability. At this particular station and sampling period (i.e., Patuxent River in 2004), computations using the high-frequency data (DHO=May 21, ROD=6.05 mmol m⁻³ day⁻¹) and fortnightly observations (DHO=May 22, ROD=5.24 mmol m⁻³ day⁻¹) are comparable, suggesting that fortnightly data reasonably reflect broad regional and seasonal patterns of O₂ declines.

Longer term variability in the distribution of O₂ reveals seasonally shifting controls on O₂ consumption. During March and April in the upper region of Chesapeake Bay where O₂ depletion first occurs, the standard deviation of the 1985–2009 mean is highest in deeper water (Fig. 5b), where accumulations of chlorophyll *a* commonly develop (data not shown) just seaward of the limit of salt intrusion (Sanford et al. 2001). This region is also within the estuarine turbidity maximum, where organic matter and phytoplankton may be concentrated (Lee et al. 2012). In contrast, variability during May and especially June is highest at mid-depth in the middle

region of Chesapeake Bay. Such variability may be due to fluctuations in pycnocline location, which commonly occurs around 10 m depth and is characterized by strong gradients in O₂ (Murphy et al. 2011). Alternatively, thin layers and/or oxic/anoxic interfaces at or near the pycnocline have been found to be hot spots for particle aggregation and microbial metabolism (Durham and Stocker 2012), potentially driving O₂ variation via oxic respiration or chemautotrophy associated with sulfide or ammonium oxidation (Casamayor et al. 2001). This spatial pattern in the primary controlling mechanisms of O₂ variability (i.e., organic matter availability in the upper Bay, stratification strength in the lower Bay) is consistent with the statistical analysis of interannual variability in DHO and ROD (Tables 3 and 4).

Interannual Variability in O₂ Depletion

Interannual variation in freshwater input is an important driver of biogeochemical processes in estuarine ecosystems, including O₂ depletion. Although Susquehanna River flow is statistically the strongest predictor of DHO and ROD at some stations (CB3.3C–CB5.1; Tables 3 and 4), flow impacts both the biology and physics of Chesapeake Bay, and these effects

Table 3 Table of correlation coefficients (*r*; top value) and associated *p* values (bottom value) for correlations between the date of hypoxia onset (DHO) and potential controlling variables, including Susquehanna River flow, April–May Brunt–Väisälä frequency, and bottom chlorophyll *a* concentration

Hypoxia onset	CB3.3C (<i>n</i> =25)	CB4.1C (<i>n</i> =25)	CB4.2C (<i>n</i> =25)	CB4.3C (<i>n</i> =25)	CB4.4 (<i>n</i> =25)	CB5.1 (<i>n</i> =25)	CB5.2 (<i>n</i> =25)	CB5.3 (<i>n</i> =25)	CB5.4 (<i>n</i> =24)	CB5.5 (<i>n</i> =21)	CB6.1 (<i>n</i> =19)	CB6.2 (<i>n</i> =13)
Susquehanna flow (January–March)	-0.69 <0.001	-0.57 0.003	-0.54 0.006	-0.55 0.005	-0.47 0.019	-0.54 0.006	-0.36 0.074	-0.29 0.162	-0.14 0.512	-0.18 0.442	-0.14 0.563	-0.002 0.995
Susquehanna flow (February–April)	-0.38 0.059	-0.51 0.009	-0.64 0.001	-0.63 0.001	-0.58 0.003	-0.60 0.002	-0.35 0.082	-0.35 0.086	-0.31 0.142	-0.23 0.315	-0.26 0.286	-0.37 0.220
Chlorophyll <i>a</i> (January–April)	-0.53 0.007	-0.73 <0.001	-0.62 0.001	-0.61 0.001	-0.52 0.008	-0.42 0.036	-0.47 0.018	-0.21 0.310	-0.18 0.399	-0.48 0.034	-0.42 0.081	-0.23 0.456
Brunt–Väisälä frequency (April)	0.40 0.048	-0.13 0.536	-0.10 0.626	-0.15 0.478	-0.16 0.430	-0.19 0.354	-0.38 0.059	-0.21 0.315	-0.64 0.001	-0.24 0.286	0.29 0.223	-0.06 0.855
Brunt–Väisälä frequency (May)	0.08 0.715	-0.03 0.890	-0.32 0.114	-0.22 0.280	-0.07 0.753	-0.19 0.364	-0.37 0.066	-0.36 0.080	-0.53 0.010	-0.29 0.211	-0.50 0.036	-0.28 ^a 0.360

For each controlling variable, two periods of aggregation are included. Numbers in italics indicate significance (*p*<0.05)

^a Date of hypoxia onset at this station was significantly correlated to regional mean (CB5.4–CB6.4) of the given variable

Table 4 Table of correlation coefficients (*r*; top value) and associated *p* values (bottom value) for correlations between the March to May water column O₂ depletion rate (ROD) and potential controlling variables,including Susquehanna River flow, Brunt–Väisälä frequency, water temperature, and bottom chlorophyll *a* concentration

O ₂ depletion rate	CB3.3C (<i>n</i> =25)	CB4.1C (<i>n</i> =25)	CB4.2C (<i>n</i> =25)	CB4.3C (<i>n</i> =24)	CB4.4 (<i>n</i> =25)	CB5.1 (<i>n</i> =25)	CB5.2 (<i>n</i> =25)	CB5.3 (<i>n</i> =25)	CB5.4 (<i>n</i> =20)	CB5.5 (<i>n</i> =22)	CB6.1 (<i>n</i> =23)	CB6.2 (<i>n</i> =22)
Susquehanna flow (January–March)	−0.20 0.345	−0.12 0.580	0.03 0.870	0.29 0.168	0.26 0.218	0.30 0.143	0.36 0.075	−0.12 0.561	−0.19 0.422	−0.10 0.669	−0.04 0.855	0.04 0.860
Susquehanna flow (February–April)	0.07 0.745	0.28 0.190	<i>0.40</i> <i>0.048</i>	<i>0.50</i> <i>0.012</i>	<i>0.45</i> <i>0.025</i>	<i>0.45</i> <i>0.023</i>	0.38 0.060	0.14 0.496	0.03 0.889	0.13 0.560	0.08 0.709	0.19 0.390
Chlorophyll <i>a</i> (January–April)	−0.14 0.496	−0.003 0.990	<i>0.43</i> <i>0.030</i>	<i>0.51^a</i> <i>0.011</i>	<i>0.48^a</i> <i>0.014</i>	0.34 0.092	<i>0.43^a</i> <i>0.032</i>	0.23 0.275	0.35 0.126	0.12 0.593	0.22 0.323	0.35 0.112
Brunt–Väisälä frequency (April)	0.33 0.112	0.28 0.189	0.12 0.578	0.004 0.985	0.004 0.984	0.057 0.784	<i>0.47</i> <i>0.017</i>	0.12 0.580	0.13 0.591	0.08 0.722	−0.05 0.825	−0.25 0.258
Brunt–Väisälä frequency (May)	−0.24 0.248	0.18 0.393	0.23 0.269	0.18 0.407	0.17 0.405	0.30 ^a 0.150	<i>0.46^a</i> <i>0.021</i>	0.25 0.220	0.16 0.503	0.33 0.139	<i>0.53</i> <i>0.009</i>	0.39 0.074

For each controlling variable, two periods of aggregation are included. Numbers in italics indicate significance ($p < 0.05$)

^a Water column O₂ depletion rate at these stations was significantly correlated to regional means (CB4.3C–CB5.2) of the given variable

cannot be satisfactorily isolated with simple statistics. The effect of flow on interannual variability in the development and spatial–temporal extent of O₂-depleted waters is a result of flow impacts on a suite of biological and physical variables, including the magnitude of the spring diatom bloom, spring water temperature, and associated vertical and horizontal O₂ transport (e.g., Hagy et al. 2004; Officer et al. 1984; Taft et al. 1980). For example, elevated winter–spring river flow should favor O₂ depletion by increasing stratification strength (Boicourt 1992) and elevating phytoplankton biomass (Boynton and Kemp 2000; Malone et al. 1988). Elevated flow may, however, increase O₂ concentrations via enhanced landward, longitudinal O₂ transport (Kemp et al. 1992). High flow also tends to push the location of the spring bloom seaward (e.g., Hagy et al. 2005), which should increase ROD in lower Bay regions. ROD was indeed elevated in mid-Bay regions during high-flow years (Fig. 7), suggesting that the O₂-depleting effects of elevated organic material and stratification strength may outweigh the O₂-replenishment effects of enhanced longitudinal advection, at least in the mid-Bay region. Either way, strong correlations between river flow and DHO/ROD reveal that future changes in precipitation will likely impact the phenology of hypoxia development in Chesapeake Bay.

To avoid interpretation problems associated with the covariability of freshwater flow and with various biological and physical processes, we focused our analysis on variables that directly represent the functional effect of flow within the estuary (phytoplankton biomass and stratification strength). Winter–spring O₂ depletion metrics appear to be driven primarily by phytoplankton-derived organic matter in the upper and middle regions of the Bay. DHO and ROD were most

strongly linked to chlorophyll *a* in bottom water, where phytoplankton biomass tends to accumulate during the winter–spring period (data not shown). Statistical analyses from this study (Tables 3 and 4), as well as previous studies of O₂ dynamics in Chesapeake Bay (e.g., Boynton and Kemp 2000) support this assertion. Substantial phytoplankton biomass accumulations associated with the winter–spring bloom (Harding and Perry 1997; Malone et al. 1988) are associated with low grazing rates (White and Roman 1992) and high deposition rates of fresh organic material (Kemp et al. 1999). As temperature begins to rise in spring, high POC concentrations result in elevated respiration and rapid rates of O₂ uptake (Malone 1987; Sampou and Kemp 1994). Indeed, O₂ depletion rates in Chesapeake Bay were significantly related to chlorophyll *a* deposition rates derived from sediment traps over the course of several years (Boynton and Kemp 2000), and biomarker studies indicate that sediment organic matter is most labile during the spring bloom (Zimmerman and Canuel 2001). Thus, there is strong evidence for the association of winter–spring O₂ declines with the bottom water biomass of phytoplankton over a large section of Chesapeake Bay.

Although the relationships between bottom water chlorophyll *a* and both ROD and DHO are strong in several regions of the Bay, we do not presume that physical transport effects are small. Several investigators have illustrated the importance of stratification, lateral advection and mixing, and longitudinal advection as important controls on O₂ distribution in Chesapeake Bay (Goodrich et al. 1987; Li and Li 2011; Sanford and Boicourt 1990; Scully 2010). Correlation analysis reveals that stratification strength is the strongest predictor of hypoxia onset and O₂ depletion at several stations in the

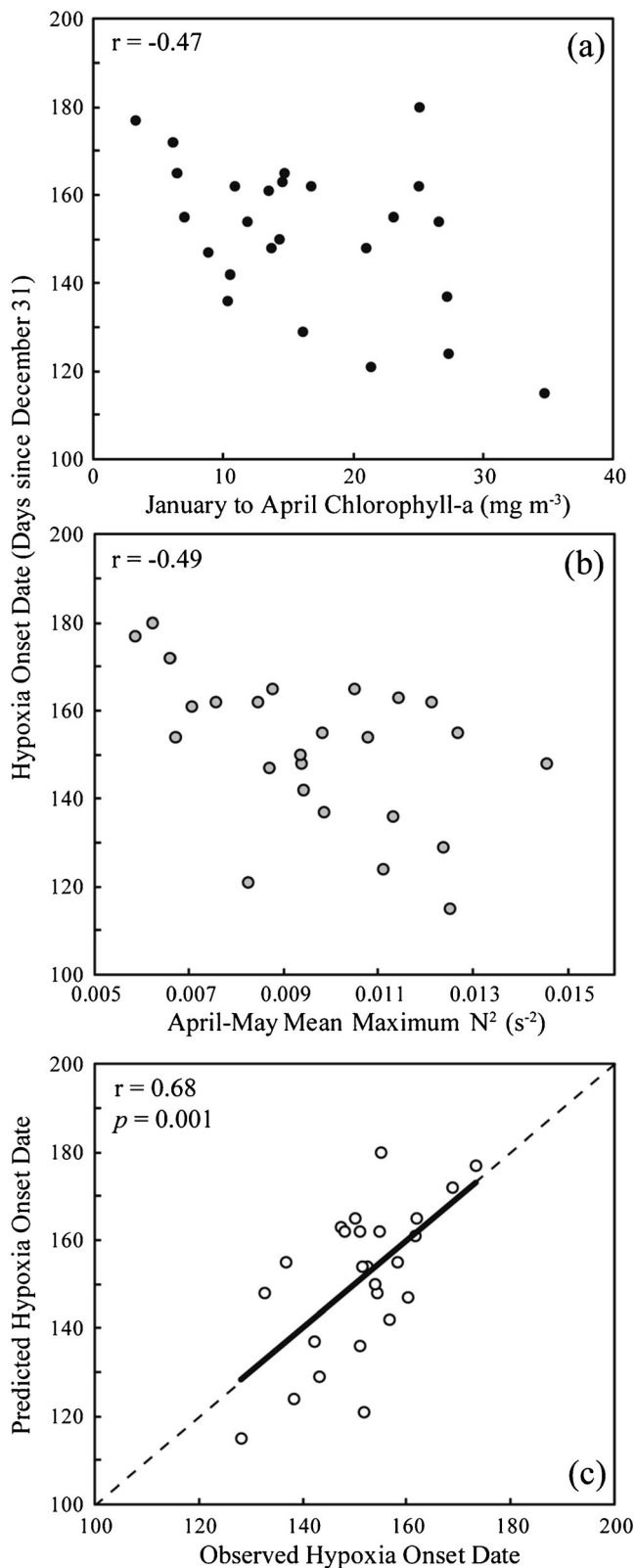


Fig. 8 Correlations of **a** January to April bottom water phytoplankton biomass (chlorophyll *a*) and **b** April to May mean stratification strength (Brunt–Väisälä frequency, N^2) with date of hypoxia onset at station CB5.2 (see Fig. 1). **c** Observed date of hypoxia onset plotted against predictions from a multiple linear regression with chlorophyll *a* and N^2

middle and lower Bay, and the highest variability in summer O_2 concentrations occurs within or adjacent to the pycnocline (Fig. 5b). Stratification strength may be a larger contributor to ROD and DHO in more seaward reaches of the Bay because phytoplankton biomass (Harding and Perry 1997) and deposition (Hagy et al. 2005) tend to be lower in this region, thus limiting the biological influence on O_2 depletion. Physical mechanisms may also be of greater importance in summer, when stratification strength reaches its seasonal maxima and vertical gradients of O_2 are stronger, at several middle and lower Bay stations (Murphy et al. 2011). Consequently, associations of vertical mixing with hypoxia may be stronger in the lower Bay, where hypoxia onset occurs later in the year when stratification strength is at or near its peak (e.g., June, Fig. 6) (Table 3).

Although there has been limited use of hydrographic data to estimate rates of oxygen consumption in estuaries, there is a long history of such analyses in lake and open ocean research. In lakes, the hypolimnetic oxygen deficit (or hypolimnetic oxygen depletion rate) has long been used as a metric of productivity for evaluating trophic status and for inter-system comparisons (e.g., Burns et al. 2005; Matthews and Effler 2006; Rosa and Burns 1987). In open ocean research, apparent oxygen utilization has been used to estimate the O_2 consumption due to biochemical processes relative to a preformed value, which is often the solubility O_2 concentration (e.g., Garcia et al. 2005; Pytkowicz 1971). Both metrics utilize relatively easy-to-collect hydrographic data to derive rates and indices of biogeochemical O_2 uptake, similar to the ROD methods reported in this paper. Interestingly, long-term (1970–2003) estimates of hypolimnetic volume-corrected oxygen depletion in Lake Erie range from 2.4 to 4.9 $mmol O_2 m^{-3} day^{-1}$ (Burns et al. 2005), which are less variable, but comparable to ROD reported in this study (Table 2). Although the reason for higher variation in Chesapeake Bay ROD is unclear, this comparison reveals similarities in the rate in which deep-water O_2 is depleted in enriched aquatic ecosystems, and emphasizes the utility of such approaches across ecosystems.

Winter–Spring O_2 Depletion and Summer Hypoxic Volume

Our metrics of spring O_2 depletion rates and dates generally do not correlate with the volume of hypoxic bottom water in the subsequent summer. The only significant correlations that we did find were between late spring (May 1–June 15) hypoxic volumes and DHO/ROD in mid-Bay regions. This suggests that the influence of the winter–spring bloom on hypoxic volume weakens substantially as summer progresses and the spring bloom decomposes. Mid-to-late summer hypoxic volumes were, however, not correlated with DHO and ROD for most Bay regions analyzed, and summer hypoxic volume

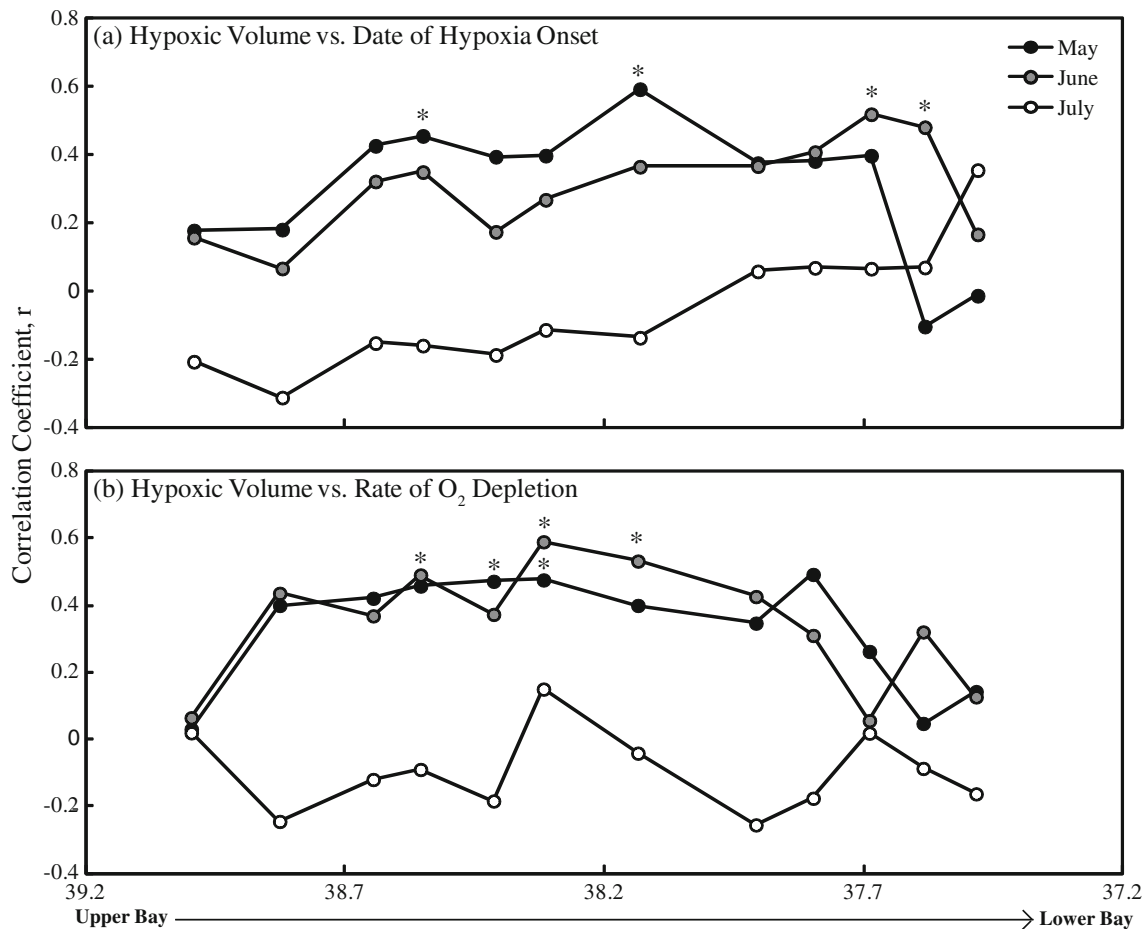


Fig. 9 Correlation coefficient (r) for relationships between hypoxic volume (during the latter half of May, June, and July) and **a** hypoxia onset day and **b** rates of water column O_2 depletion as they vary along the main Chesapeake Bay. Asterisks near the circles indicate significant correlations

appears to be a dynamic feature that varies with summer phytoplankton production (Testa 2013) and climatic conditions (Feng et al. 2012; O'Donnell et al. 2008; Scully 2010). One important implication of this observed disconnect between spring and summer O_2 conditions is that, in contrast to previous inferences that the spring bloom fuels summer hypoxia (e.g., Malone 1987; Pomeroy et al. 2006), it appears that a large spring bloom does not guarantee large summer hypoxic volumes. This conclusion is supported by various calculations and modeling experiments, which suggest that labile organic matter from spring phytoplankton is largely depleted by summer and that contemporaneous phytoplankton production is necessary for sustained summer hypoxic conditions in Chesapeake Bay (Newell et al. 2007; Testa 2013).

The fact that we did find significant relationships between winter–spring flow and DHO/ROD, but found no such relationship between DHO/ROD and summer hypoxic volume might seem inconsistent with previous reports. For example, strong statistical relationships have been reported for winter–spring flow (and/or TN load) versus summer hypoxic volume (Hagy et al. 2004; Lee et al. 2013; Scavia et al. 2006).

Although we did find significant correlations between spring O_2 decline (DHO/ROD) and late spring hypoxia, we found no relationship with summer hypoxia. These findings indicate that there is a diminishing connection between spring O_2 consumption and the volume of hypoxic water that can be maintained over the course of the summer. Previous studies that have found strong relationships between winter–spring flow (or nutrient loading) and summer hypoxia used temporally integrated measures of hypoxia, including means over the month of July (Hagy et al. 2004; Scavia et al. 2006) or warm-season means (Lee et al. 2013). In contrast, our analysis examined correlations between DHO/ROD and cruise-specific hypoxic volumes computed from data collected at 1–2 week intervals, and recent analyses have revealed that volume and temporal patterns of hypoxia vary systematically from late spring to late summer (Murphy et al. 2011). Thus, we emphasize that the relationships between winter–spring flow (or nutrient loading) and summer hypoxic volume are complex and that further analyses are needed to resolve details of the associated spatial and temporal dynamics of O_2 depletion in Chesapeake Bay.

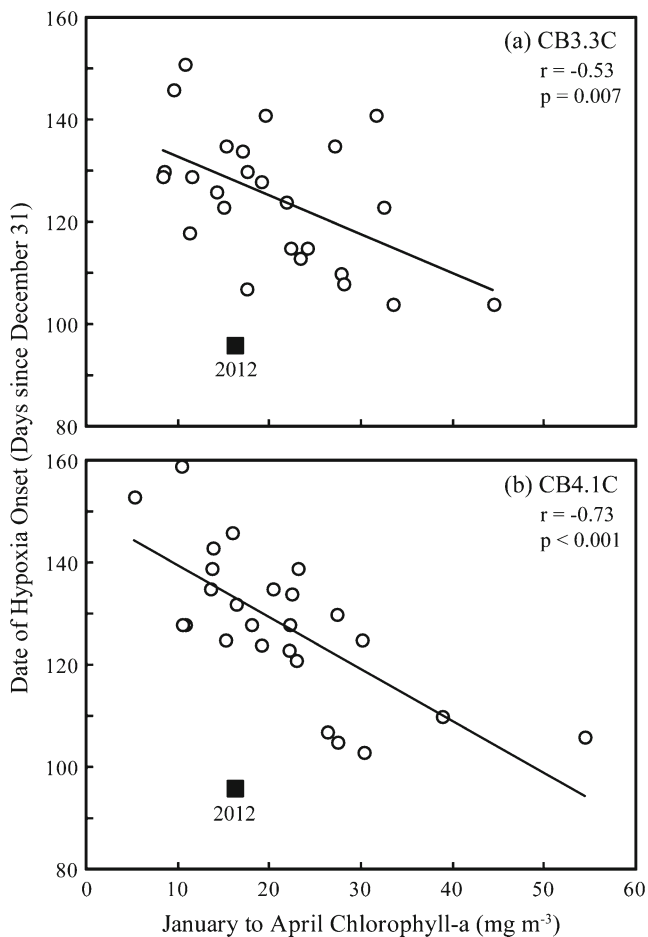


Fig. 10 Correlations between January to April bottom water chlorophyll *a* and the date of hypoxia onset (DHO) at stations **a** CB3.3C and **b** CB4.1C for the 1985–2009 period (*open circles*) and for the year 2012 (*closed square*)

Winter–Spring O₂ Depletion in 2012

The onset of hypoxia in upper Chesapeake Bay in 2012 (April 6) occurred 8 days before the earliest onset dates from the previous 26 years (Fig. 10). The April 6 hypoxia onset was also much earlier than expected from January to April bottom water chlorophyll *a* at stations CB3.3C and CB4.1C, given patterns from the previous decades (Fig. 10). This seemingly unusual pattern in 2012 presents a useful case study for understanding the controls on winter–spring O₂ depletion. The passing of Tropical Storm Lee over much of the Susquehanna River watershed in September of 2011 resulted in extraordinary levels of freshwater flow and the highest suspended sediment loads to Chesapeake Bay recorded in 30 years (Hirsch 2012). Although the lability and character of this material is uncertain at this time, modeling studies suggest that large amounts of clay and silt material were deposited to sediments in much of the upper Bay (Cheng et al. 2013). Previous investigators have speculated that

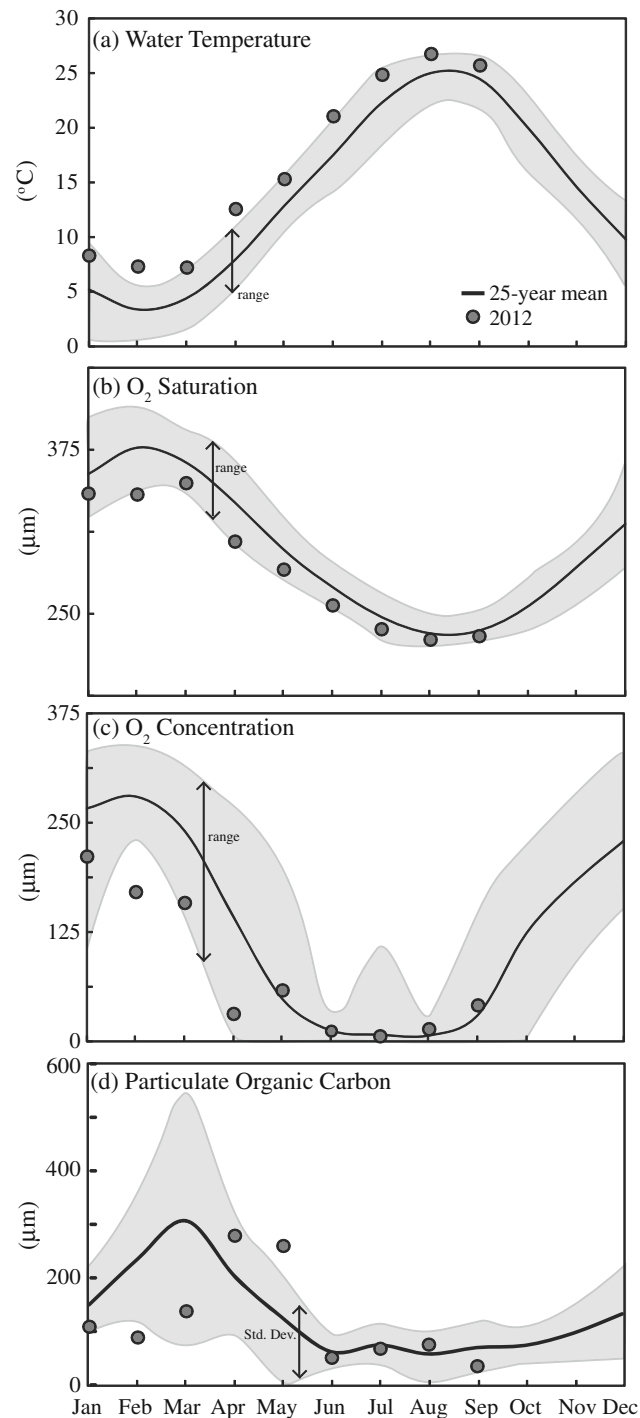


Fig. 11 Seasonal cycles of monthly mean water quality conditions in the bottom waters over 1985–2009 at station CB3.3C in Chesapeake Bay (see Fig. 1): for **a** temperature; **b** oxygen solubility; **c** O₂ concentration; and **d** particulate organic carbon (POC). Mean values are shown as a *solid line*, the *shaded area in the top three panels* shows the range (i.e., 25-year maximum and minimum value for each respective month), and the *shaded area in the bottom panel* (i.e., POC) is the 25-year standard deviation (SD was used because maximum values were highly variable). *Filled circles* are observations from 2012

organic material deposited to sediments in autumn might remain intact in sediments over the winter (due to low

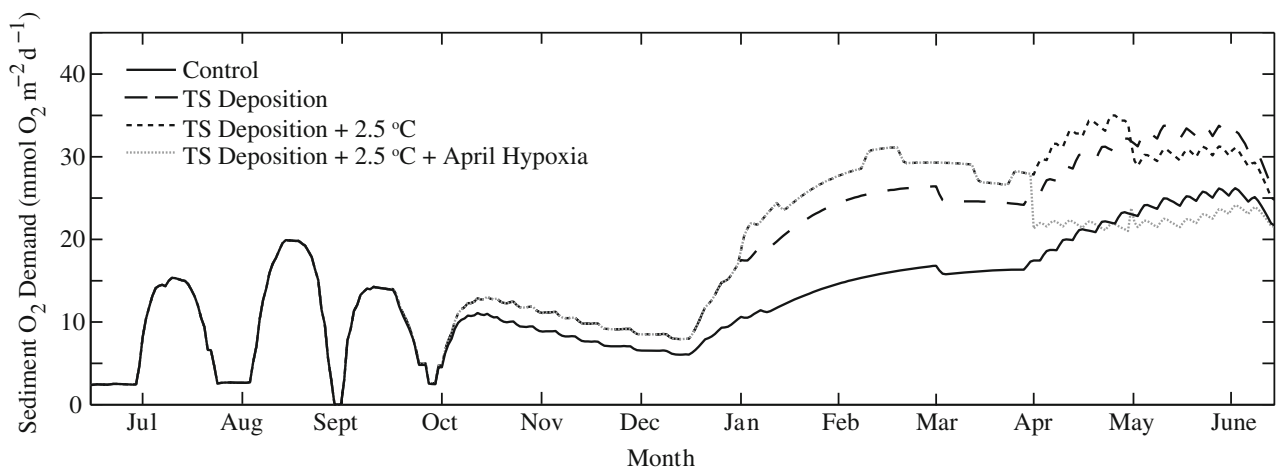


Fig. 12 Time series of sediment O_2 demand (SOD) from July to July in a simulation experiment with a two-layer sediment biogeochemical model (Brady et al. 2013) at station CB3.3C in Chesapeake Bay. The *black line* represents the “control” experiment, based on average conditions, the *large dashed line* represents the model forced with a month-long

elevation of POM deposition representing the impact of Tropical Storm Lee in September 2011, the *small dashed line in black* represents the TS Lee experiment with January to April temperatures elevated by 2.5 °C, and the *gray dotted line* represents the TS Lee+Temperature experiment with hypoxia beginning on April 1

temperatures) and be respired in the following spring (e.g., Boynton and Kemp 2000; Taft et al. 1980).

Observations of bottom water-dissolved O_2 at several stations in the upper and middle Bay were at record low levels in the winter–spring of 2012. Although water temperature was historically high during these months (2.1 °C above long-term maximum), associated declines in solubility do not explain the observed low O_2 concentrations (Fig. 11a, b). Stratification strength approached the 26-year maxima at stations CB3.3C and CB4.1 during this period (0.01–0.015 s^{-2}), suggesting that high stratification due to low wind stress during March (data not shown) could have led to reduced O_2 . An alternative (or additional) explanation is that respiration of elevated levels of organic matter was responsible. Indeed, POC and chlorophyll *a* concentrations in the bottom water at stations CB3.3C and CB4.1C were 1.5 to 2 times the long-term mean in April 2012 (e.g., Fig. 11). Such large pools of POC at these stations, in addition to elevated temperatures to enhance respiration rates (Fig. 11a; Sampou and Kemp 1994), suggest that water column respiration was elevated during winter–spring 2012.

An alternative, yet difficult to assess contributor to reduced O_2 concentrations in 2012 is elevated sediment O_2 demand (SOD) resulting from carry-over of organic matter inputs from the previous fall. Previous modeling of sediment biogeochemistry in Chesapeake Bay suggested that labile organic material deposition from the previous year can accumulate and carry-over to the following spring (Brady et al. 2013). We applied a two-layer sediment flux model (Brady et al. 2013; Testa et al. 2013) to examine the seasonal response of sediments to a large September depositional event, where a month-long pulse of POM (equivalent to 30 % of the total annual POM flux) was simulated. Although this simulation may be conservative relative to the overall delivery of particulate material to the Bay

(Cheng et al. 2013), it reflects the fact that some of the material delivered during the storm is recalcitrant and that much of it was delivered to sediments north of CB3.3C. Four total simulations were run, including (1) a control, where fall POM deposition was equivalent to the long-term mean, (2) the month-long, elevated POM flux representing TS Lee, (3) the elevated POM flux with temperatures elevated by 2.5 °C in the following January to April period, and (4) simulation #3 with dissolved O_2 reduced to hypoxic conditions (47 $\mu M O_2$) beginning on April 1 of the following year (Fig. 12). Runs #3 and #4 are consistent with observed water column conditions in 2012. Organic matter diagenesis rates for all organic matter pools were set to 0.01 day^{-1} , which is consistent with moderately labile organic matter (Burdige 1991; Westrich and Berner 1984).

The simulations suggest that a depositional event associated with a large autumn depositional event, combined with high observed water temperatures, could have doubled SOD in the following winter–spring period, from 15 to 30 $mmol O_2 m^{-2} day^{-1}$ (Fig. 12). The effect of the observed early onset of hypoxia in the beginning of April reduced SOD by roughly 30 %, resulting in SOD comparable to that predicted in the control run after April 1 (Fig. 12). However, SOD likely only contributes 10 % of total sub-pycnocline O_2 demand at station CB3.3C, given a ~20 m aphotic water column with water column respiration rates of 15 $mmol O_2 m^{-3} day^{-1}$ (Sampou and Kemp 1994) and SOD rates of 30 $mmol O_2 m^{-3} day^{-1}$. SOD may have been a larger contributor to respiration and O_2 decline, however, in more northerly stations (north of CB3.3C), which tend to be shallow (5–15 m) and received the largest loads of POM from TS Lee (Cheng et al. 2013).

Thus, we conclude that the unusually early hypoxia onset in upper Chesapeake Bay in 2012 was likely due to the

synergistic effects of high stratification, elevated temperature, elevated POC availability in early April, and a carryover of organic material from the fall of 2011. To more realistically address this hypothesis, however, analyses should involve coupled physical–biological model simulations to separate effects of physical circulation from water column and benthic biogeochemical processes. Such a model would compute both water column and sediment responses to the loads from TS Lee if coupled to a sediment transport model (Cheng et al. 2013) and would allow a more quantitative assessment of how climatic changes (e.g., river flow, temperature) and the biogeochemical processes they influence (e.g., spring bloom timing and magnitude) influence the rate of O₂ depletion and the phenology of hypoxia development over several decades.

Conclusions

The present study provides a novel synthesis of water column O₂ depletion rates and the date of hypoxia onset for 25 years in Chesapeake Bay, describing regional and seasonal patterns of O₂ depletion over the winter–spring transition. We found clear spatial patterns in both DHO and ROD along the central axis of Chesapeake Bay, despite substantial interannual variability. These analyses illustrates that bottom water, winter–spring chlorophyll *a* was the strongest single predictor of O₂ depletion rates and hypoxia onset dates, illustrating the importance of spring bloom-derived organic material in fueling the respiration that initiates hypoxic conditions. Stratification was an important control in seaward Bay regions. The absence of significant correlation between winter–spring O₂ depletion and summer hypoxic volumes suggests that summer phytoplankton production is needed to sustain summer hypoxic volumes and that climatic variations in later spring and summer are strong controls on hypoxic volume. A record early initiation of hypoxia in the upper Bay in 2012 may have been caused by extraordinary winter–spring climatic and biological conditions and the carryover of large organic matter loads associated with a tropical storm in September 2011. This indicates the potential for both proximal and remote controls on hypoxia initiation. Thus, the phenology of hypoxia initiation in Chesapeake Bay may shift with future changes in winter precipitation and temperature patterns, as well as tropical storm activity during late summer and fall.

Acknowledgments This study was funded by the United States National Oceanographic and Atmospheric Administration (NOAA) Coastal Hypoxia Research Program (CHRP-NAO7NOS4780191), the National Science Foundation-funded Chesapeake Bay Environmental Observatory (CBEO-3 BERS-0618986), the State of Maryland Department of Natural Resources (K00B920002), and the Horn Point Laboratory Bay and Rivers Graduate Fellowship. We would like to thank the EPA Chesapeake Bay Program and the Maryland Department of Natural Resources for providing monitoring data; Rebecca

Murphy for help and support in interpolation approaches; Randall Burns and Eric Perlman for development, maintenance, and support of the CBEO testbed; William Ball, Walter Boynton, Damian Brady, Dominic Di Toro, and Jeff Cornwell for many insightful discussions. This work is NOAA Coastal Hypoxia Research Program (CHRP) Publication # 186 and the University of Maryland Center for Environmental Science Publication # 4849.

References

- Boicourt, W.C. 1992. Influences of circulation processes on dissolved oxygen in the Chesapeake Bay. In *Oxygen dynamics in the Chesapeake Bay, a synthesis of recent research*, ed. D.E. Smith, M. Lefler, and G. Mackieman, 7–59. College Park: Maryland Sea Grant.
- Boynton, W.R., and W.M. Kemp. 2000. Influence of river flow and nutrient loads on selected ecosystem processes: a synthesis of Chesapeake Bay data. In *Estuarine science: a synthetic approach to research and practice*, ed. J.E. Hobbie, 269–298. Washington DC: Island Press.
- Brady, D.C., T.E. Targett, and D.M. Tuzzolino. 2009. Behavioral responses of juvenile weakfish (*Cynoscion regalis*) to diel-cycling hypoxia: swimming speed, angular correlation, expected displacement, and effects of hypoxia acclimation. *Canadian Journal of Fisheries and Aquatic Sciences* 66: 415–424.
- Brady, D.C., J.M. Testa, D.M.D. Toro, W.R. Boynton, and W.M. Kemp. 2013. Sediment flux modeling: calibration and application for coastal systems. *Estuarine, Coastal and Shelf Science* 117: 107–124.
- Breitburg, D.L. 1990. Near-shore hypoxia in the Chesapeake Bay: patterns and relationships among physical factors. *Estuarine, Coastal and Shelf Science* 30: 593–609.
- Breitburg, D.L. 2002. Effects of hypoxia, and the balance between hypoxia and enrichment, on coastal fishes and fisheries. *Estuaries* 25: 767–781.
- Burdige, D.J. 1991. The kinetics of organic matter mineralization in anoxic marine sediments. *Journal of Marine Research* 49: 727–761.
- Burns, N.M., D.C. Rockwell, P.E. Bertram, D.M. Dolan, and J.J.H. Ciborowski. 2005. Trends in temperature, Secchi depth, and dissolved oxygen depletion rates in the central basin of Lake Erie, 1983–2002. *Journal of Great Lakes Research* 31: 35–49.
- Casamayor, E.O., J. García-Cantizano, J. Mas, and C. Pedrós-Alió. 2001. Primary production in estuarine oxic/anoxic interfaces: contribution of microbial dark CO₂ fixation in the Ebro River Salt Wedge Estuary. *Marine Ecology Progress Series* 215: 49–56.
- Cheng, P., M. Li, and Y. Li. 2013. Generation of an estuarine sediment plume by a tropical storm. *Journal of Geophysical Research-Oceans* 118: 856–868.
- Conley, D.J., C. Humborg, L. Rahm, O.P. Savchuk, and F. Wulff. 2002. Hypoxia in the Baltic Sea and basin-scale changes in phosphorus biogeochemistry. *Environmental Science and Technology* 36: 5315–5320.
- Cronin, W.B., and D.W. Pritchard. 1975. Additional statistics on the dimensions of Chesapeake Bay and its tributaries: cross-section widths and segment volumes per meter depth. Chesapeake Bay Institute, The Johns Hopkins University. Baltimore, Maryland Reference 75–3. Special Report 42. 475.
- Decker, M.B., D.L. Breitburg, and J.E. Purcell. 2004. Effects of low dissolved oxygen on zooplankton predation by the ctenophore *Mnemiopsis leidyi*. *Marine Ecology Progress Series* 280: 163–172.
- Díaz, R.J., and R. Rosenberg. 2008. Spreading dead zones and consequences for marine ecosystems. *Science* 321: 926–929.
- Durham, W.M., and R. Stocker. 2012. Thin phytoplankton layers: characteristics, mechanisms, and consequences. *Annual Review of Marine Science* 4: 177–207.

- Feng, Y., S.F. DiMarco, and G.A. Jackson. 2012. Relative role of wind forcing and riverine nutrient input on the extent of hypoxia in the northern Gulf of Mexico. *Geophysical Research Letters* 39:DOI: 10.1029/2012GL051192.
- Fofonoff, N.P. 1985. Physical properties of seawater: a new salinity scale and equation of state for seawater. *Journal of Geophysical Research* 90: 3332–3342.
- Fritsch, F.N., and R.E. Carlson. 1980. Monotone piecewise cubic interpolation. *SIAM Journal on Numerical Analysis* 17: 238–246.
- Garcia, H.E., T.P. Boyer, S. Levitus, R.A. Locarnini, and J. Antonov. 2005. On the variability of dissolved oxygen and apparent oxygen utilization content for the upper world ocean: 1955 to 1998. *Geophysical Research Letters* 32:doi:10.1029/2004GL022286.
- Goodrich, D.M., W.C. Boicourt, P. Hamilton, and D.W. Pritchard. 1987. Wind-induced destratification in Chesapeake Bay. *Journal of Physical Oceanography* 17: 2232–2240.
- Hagy, J.D., W.R. Boynton, C.W. Keefe, and K.V. Wood. 2004. Hypoxia in Chesapeake Bay, 1950–2001: long-term change in relation to nutrient loading and river flow. *Estuaries* 27: 634–658.
- Hagy, J.D., W.R. Boynton, and D.A. Jasinski. 2005. Modeling phytoplankton deposition to Chesapeake Bay sediments during winter–spring: interannual variability in relation to river flow. *Estuarine, Coastal and Shelf Science* 62: 25–40.
- Harding, L.W., and E. Perry. 1997. Long-term increase of phytoplankton biomass in Chesapeake Bay, 1950–1994. *Marine Ecology Progress Series* 157: 39–52.
- Hirsch, R.M. 2012. Flux of nitrogen, phosphorus, and suspended sediment from the Susquehanna River Basin to the Chesapeake Bay during Tropical Storm Lee, September 2011, as an indicator of the effects of reservoir sedimentation on water quality. U.S. Geological Survey. Scientific Investigations Report 2012–5185. 17 p.
- Justic, D., N.N. Rabalais, and R.E. Turner. 2005. Coupling between climate variability and coastal eutrophication: evidence and outlook for the northern Gulf of Mexico. *Journal of Sea Research* 54: 25–35.
- Kemp, W.M., P. Sampou, J. Caffrey, M. Mayer, K. Henriksen, and W.R. Boynton. 1990. Ammonium recycling versus denitrification in Chesapeake Bay sediments. *Limnology and Oceanography* 35: 1545–1563.
- Kemp, W.M., P.A. Sampou, J. Garber, J. Tuttle, and W.R. Boynton. 1992. Seasonal depletion of oxygen from bottom waters of Chesapeake Bay: roles of benthic and planktonic respiration and physical exchange processes. *Marine Ecology Progress Series* 85: 137–152.
- Kemp, W.M., S. Puskaric, J. Faganeli, E.M. Smith, and W.R. Boynton. 1999. Pelagic–benthic coupling and nutrient cycling. In *Coastal and estuarine studies, ecosystems at the land-sea margin: drainage basin to coastal sea*, ed. T.C. Malone, A. Malej, J.L.W. Harding, N. Smodlaka, and R.E. Turner, 295–339. Washington, D.C.: American Geophysical Union.
- Kemp, W.M., J.M. Testa, D.J. Conley, D. Gilbert, and J.D. Hagy. 2009. Temporal responses of coastal hypoxia to nutrient loading and physical controls. *Biogeosciences* 6: 2985–3008.
- Kuo, A.Y., K. Park, and M.Z. Moustafa. 1991. Spatial and temporal variabilities of hypoxia in the Rappahannock River, Virginia. *Estuaries* 14: 113–121.
- Lee, D.Y., D. Keller, B.C. Crump, and R.R. Hood. 2012. Community metabolism and energy transfer in the Chesapeake Bay estuarine turbidity maximum. *Marine Ecology Progress Series* 449: 65–82.
- Lee, Y., W.R. Boynton, M. Li, and Y. Li. 2013. Role of late winter–spring wind influencing summer hypoxia in Chesapeake Bay. *Estuaries and Coasts* 36: 683–696.
- Li, Y., and M. Li. 2011. Effects of winds on stratification and circulation in a partially mixed estuary. *Journal of Geophysical Research* 116: doi:10.1029/2010JC006893.
- Malone, T.C. 1987. Seasonal oxygen depletion and phytoplankton production in Chesapeake Bay: preliminary results of 1985–86 field studies. In *Dissolved oxygen in Chesapeake Bay*, ed. M. Mackiernan, 54–60. College Park: Maryland Sea Grant.
- Malone, T.C., W.M. Kemp, H.W. Ducklow, W.R. Boynton, J.H. Tuttle, and R.B. Jonas. 1986. Lateral variation in the production and fate of phytoplankton in a partially stratified estuary. *Marine Ecology Progress Series* 32: 149–160.
- Malone, T.C., L.H. Crocker, S.E. Pike, and B.W. Wendler. 1988. Influence of river flow on the dynamics of phytoplankton in a partially stratified estuary. *Marine Ecology Progress Series* 48: 235–249.
- Matthews, D.A., and S.W. Effler. 2006. Long-term changes in the areal hypolimnetic oxygen deficit (AHOD) of Onondaga Lake: evidence of sediment feedback. *Limnology and Oceanography* 51: 702–714.
- Murphy, R.M., F.C. Curriero, and W.P. Ball. 2010. Comparison of spatial interpolation methods for water quality evaluation in the Chesapeake Bay. *Journal of Environmental Engineering* 136: 160–171.
- Murphy, R.R., W.M. Kemp, and W.P. Ball. 2011. Long-term trends in Chesapeake Bay seasonal hypoxia, stratification, and nutrient loading. *Estuaries and Coasts* 34: 1293–1309.
- Nestlerode, J.A., and R.J. Diaz. 1998. Effects of periodic environmental hypoxia on predation of a tethered polychaete, *Glycera americana*: implications for trophic dynamics. *Marine Ecology Progress Series* 172: 185–195.
- Newell, R.I.E., W.M. Kemp, J.D.I. Hagy, C.F. Cerco, J.M. Testa, and W.R. Boynton. 2007. Top-down control of phytoplankton by oysters in Chesapeake Bay, USA: comment on Pomeroy et al. (2006). *Marine Ecology Progress Series* 341: 293–298.
- O'Donnell, J.H., H.G. Dam, W.F.W.F. Bohlen, W. Fitzgerald, P.S. Gray, A.E. Houk, D.C. Cohen, and M.M. Howard-Strobel. 2008. Intermittent ventilation in the hypoxic zone of western Long Island Sound during the summer of 2004. *Journal of Geophysical Research* 113: 1–13.
- Officer, C.B., R.B. Biggs, J.L. Taft, E. Cronin, M.A. Tyler, and W.R. Boynton. 1984. Chesapeake Bay anoxia: origin, development and significance. *Science* 223: 22–27.
- Pomeroy, L.R., C.F. D'Elia, and L.C. Schaffner. 2006. Limits to top-down control of phytoplankton by oysters in Chesapeake Bay. *Marine Ecology Progress Series* 325: 301–309.
- Pond, S., and G.L. Pickard. 1983. *Introductory dynamical oceanography*, 2nd. Oxford, UK: Butterworth-Heinemann.
- Pytkowicz, R.M. 1971. On the apparent oxygen utilization and the preformed phosphate in the oceans. *Limnology and Oceanography* 16: 39–42.
- R Development Core Team. 2009. The R project for statistical computing. <http://www.r-project.org/>. Accessed 15 Feb 2013.
- Rabalais, N.N., and D. Gilbert. 2009. Distribution and consequences of hypoxia. In *Watersheds, bays and bounded seas*, ed. E. Urban, B. Sundby, P. Malanotte-Rizzoli, and J.M. Melillo, 209–226. Washington, D.C.: Island Press.
- Ribeiro, P.J., and P.J. Diggle. 2009. geoR: A package for geostatistical analysis using the R software. <http://leg.ufpr.br/geoR/>. Accessed 15 Feb 2013.
- Rosa, F., and N.M. Burns. 1987. Lake Erie central basin oxygen depletion changes from 1929–1980. *Journal of Great Lakes Research* 13: 684–696.
- Sampou, P., and W.M. Kemp. 1994. Factors regulating plankton community respiration in Chesapeake Bay. *Marine Ecology Progress Series* 110: 249–258.
- Sanford, L.P., and W.C. Boicourt. 1990. Wind-forced salt intrusion into a tributary estuary. *Journal of Geophysical Research* 95: 13357–13371.
- Sanford, L.P., S.E. Suttles, and J.P. Halka. 2001. Reconsidering the physics of the Chesapeake Bay estuarine turbidity maximum. *Estuaries* 24: 655–669.

- Scavia, D., E.L.A. Kelly, and J.D. Hagy. 2006. A simple model for forecasting the effects of nitrogen loads on Chesapeake Bay hypoxia. *Estuaries and Coasts* 29: 674–684.
- Scully, M.E. 2010. Wind modulation of dissolved oxygen in Chesapeake Bay. *Estuaries and Coasts* 33: 1164–1175.
- Taft, J.L., W.R. Taylor, E.O. Hartwig, and R. Loftus. 1980. Seasonal oxygen depletion in Chesapeake Bay. *Estuaries* 3: 242–247.
- Testa, J.M. 2013. *Dissolved oxygen and nutrient cycling in Chesapeake Bay: an examination of controls and biogeochemical impacts using retrospective analysis and numerical models*. College Park: University of Maryland.
- Testa, J.M., and W.M. Kemp. 2012. Hypoxia-induced shifts in nitrogen and phosphorus cycling in Chesapeake Bay. *Limnology and Oceanography* 57: 835–850.
- Testa, J.M., D.C. Brady, D.M.D. Toro, W.R. Boynton, J.C. Cornwell, and W.M. Kemp. 2013. Sediment flux modeling: nitrogen, phosphorus and silica cycles. *Estuarine, Coastal and Shelf Science* 131: 245–263.
- Vaquier-Sunyer, R., and C.M. Duarte. 2008. Thresholds of hypoxia for marine biodiversity. *Proceedings of the National Academy of Sciences of the United States of America* 105: 15452–15457.
- Westrich, J.T., and R.A. Berner. 1984. The role of sedimentary organic matter in bacterial sulfate reduction: the G Model tested. *Limnology and Oceanography* 29: 236–249.
- White, J.R., and M.R. Roman. 1992. Seasonal study of grazing by metazoan zooplankton in the mesohaline Chesapeake Bay. *Marine Ecology Progress Series* 86: 251–261.
- Wilson, R.E., R.L. Swanson, and H.A. Crowley. 2008. Perspectives on long-term variations in hypoxia conditions in western Long Island Sound. *Journal of Geophysical Research* 113: doi: [10.1029/2007JC004693](https://doi.org/10.1029/2007JC004693).
- Zimmerman, A.R., and E.A. Canuel. 2001. Bulk organic matter and lipid biomarker composition of Chesapeake Bay surficial sediments as indicators of environmental processes. *Estuarine, Coastal and Shelf Science* 53: 319–341.